Fundamentals of Blackbody Radiation

Prof. Elias N. Glytsis

March 28, 2023

School of Electrical & Computer Engineering
National Technical University of Athens

This page was intentionally left blank......

Contents

1 Introduction and Electromagnetic Modes Density

A blackbody is an idealized physical body that can absorb all incident electromagnetic radiation independently of its frequency and its angle of incidence. At thermal equilibrium a blackbody emits all absorbed radiation. The re-emitted radiation energy depends only on its temperature. Therefore the intensity of the emitted radiation is related to the amount of energy in the body at thermal equilibrium. The history of the development of the theory of the blackbody radiation is very interesting since it led to the discovery of the quantum theory [1]. Josef Stefan, Ludwig Boltzmann, Wilhelm Wien, and finally Max Planck were instrumental in the development of the theory of blackbody radiation. A nice summary of their short biographies and the methodologies that were used to obtain their results is presented by Crepeau [2].

Early experimental studies established that the emissivity of a blackbody is a function of frequency and temperature. A measure of the emissivity can be the term $\rho(\nu, T)$ which is the density of radiation energy per unit volume per unit frequency (J/m^3Hz) at an absolute temperature T and at frequency ν. The first theoretical studies used the very successful at that point theory of Maxwell equations for the determination of the density of electromagnetic modes and from that the determination of $\rho(\nu, T)$. For example, Wilhelm Wien in 1896 used a simple model to derive the expression

$$\rho(\nu, T) = \alpha\nu^3 \exp(-\beta\nu/T) \tag{1}$$

where α, β were constants. Wien used the hypothesis that radiation was emitted by molecules which followed a Maxwellian velocity distribution and that the wavelength of radiation depended only on the molecule's velocity [2]. However, the above equation failed in the low frequency range of the experimental data.

In June 1900 Lord Rayleigh published a model based on the modes of electromagnetic waves in a cavity. Each mode possessed a particular frequency and could give away and take up energy in a continuous manner. Using the standard electromagnetic theory of a cuboid cavity resonator (see Fig. 1) with perfect conductor walls the following dispersion equation can be easily obtained [3–5] (see Appendix A) :

$$\left(\frac{m\pi}{a}\right)^2 + \left(\frac{p\pi}{b}\right)^2 + \left(\frac{q\pi}{d}\right)^2 = \left(\frac{2\pi\nu}{c}\right)^2 n^2, \tag{2}$$

where n is the index of refraction of the medium, and a, b, and d are the dimensions of the cavity resonator in the x, y, and z directions, and m, p, q are positive integers.

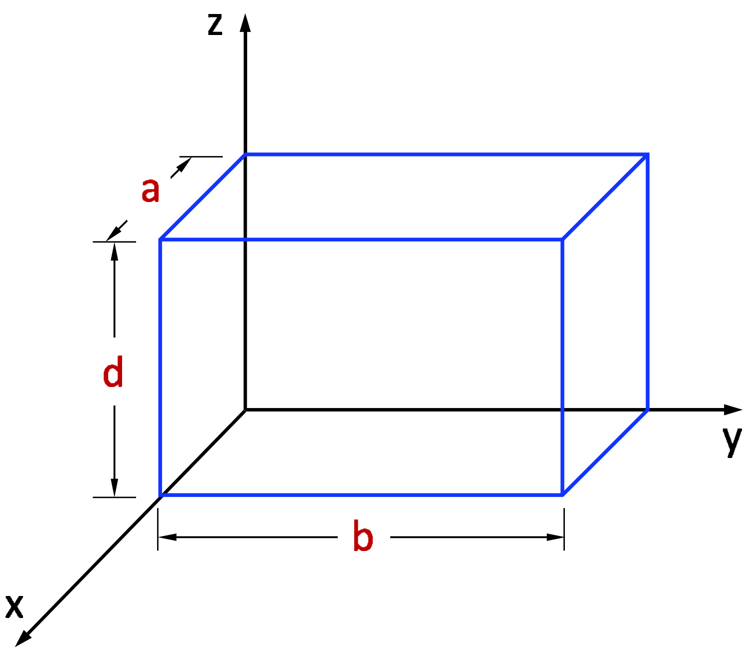

Figure 1: Cavity box (a cuboid) for the determination of the density of electromagnetic modes.

If for simplicity it is assumed that the cavity is a cube, $a = b = d$ then the previous equation can be written as

$$m^2 + p^2 + q^2 = \left(\frac{2\nu}{c}\right)^2 a^2 n^2 = \left(\frac{2\nu n a}{c}\right)^2. \tag{3}$$

In order to count the electromagnetic modes up to frequency ν it is necessary to evaluate the number of modes that fit in the one eighth of the sphere that is shown in Fig. 2 (since negative values of m, p, and q. do not represent different modes - see Appendix A). Thus, the total number of electromagnetic modes $N(\nu)$ can be determined as follows

$$N(\nu) = \frac{(1/8)\text{ cavity volume}}{\text{volume of a mode}} = \frac{(1/8)(4/3)\pi(2\nu an/c)^3}{1 \times 1 \times 1} = \frac{4}{3}\pi\frac{\nu^3 n^3 a^3}{c^3}. \tag{4}$$

Due to TE and TM mode degeneracy the above number should be multiplied by a factor of 2. Therefore, the total number of electromagnetic modes per volume, $\mathcal{N}(\nu)$, is

$$\mathcal{N}(\nu) = \frac{N(\nu)}{Volume = a^3} = \frac{8}{3}\pi\frac{\nu^3 n^3}{c^3}. \tag{5}$$

Then the density of electromagnetic modes per frequency is

$$\frac{d\mathcal{N}(\nu)}{d\nu} = \frac{8\pi\nu^2 n^3}{c^3}. \tag{6}$$

In the last equation it is assumed that the refractive index n is independent of frequency (or freespace wavelength). Usually for all materials there is dispersion, i.e. dependence of the refractive index on the frequency (or wavelength) of the electromagnetic radiation. In the latter case $n = n(\nu)$ and in the above derivative over frequency this dependence must be taken into account. Then the previous equation can be written as follows [6]

$$\frac{d\mathcal{N}(\nu)}{d\nu} = \frac{8\pi\nu^2 n^2 \left(n + \nu \dfrac{dn}{d\nu}\right)}{c^3} = \frac{8\pi\nu^2 n^2 n_g}{c^3}. \tag{7}$$

where $n_g = n + \nu(dn/d\nu) = n - \lambda_0(dn/d\lambda_0)$ (where λ_0 is the freespace wavelength) is the group refractive index and is important in materials such semiconductors and fibers where the refractive index dependence on frequency (or wavelength) can be significant. For the remainder of this section it is assumed that the refractive index is independent of frequency (or wavelength) for the sake of simplicity.

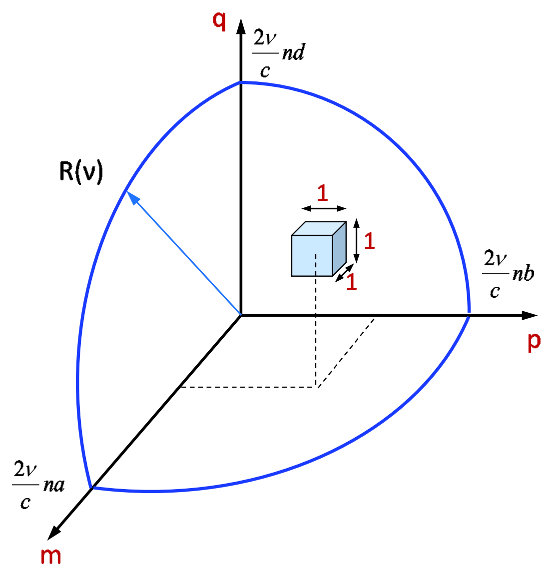

Figure 2: The one eighth of the sphere in the mpq space for the determination of the number of electromagnetic modes up to frequency ν.

2 Energy Associated with Electromagnetic Modes

Rayleigh assigned an energy $k_BT/2$ to each electromagnetic mode ($k_BT/2$ for the electric field oscillation and $k_BT/2$ for the magnetic field oscillation, where $k_B = 1.380649 \times 10^{-23} J/^\circ K$ is

Boltzmann's constant). More rigorously, the average energy of each electromagnetic mode can be determined using Boltzmann's statistics [7]. According to these statistics the probability $p(E)$ that an energy of each electromagnetic mode is between E and $E + dE$ is given by

$$p(E)dE = A \exp\left(-\frac{E}{k_B T}\right) dE, \tag{8}$$

where A is a normalization constant that can be easily found from the normalization of $p(E)$ in order to represent a probability density function. Therefore, the constant A is given by

$$\int_0^\infty p(E)dE = 1 \Longrightarrow A = \frac{1}{\displaystyle\int_0^\infty \exp(-E/k_B T)dE} = \frac{1}{k_B T}. \tag{9}$$

Then, the average energy of each electromagnetic mode can be determined from

$$\langle E \rangle = \int_0^\infty E p(E)dE = \int_0^\infty E \frac{1}{k_B T} \exp\left(-\frac{E}{k_B T}\right) dE = k_B T. \tag{10}$$

Using Eq. (6) and the average energy of Eq. (10) the electromagnetic energy density per unit frequency $\rho(\nu, T)$ becomes

$$\rho(\nu, T) = \frac{d\mathcal{N}(\nu)}{d\nu} \langle E \rangle = \frac{8\pi\nu^2 n^3}{c^3} k_B T. \tag{11}$$

The last equation is known as the Rayleigh-Jeans distribution of a blackbody radiation and fails dramatically in the ultraviolet part of the spectrum (historically referred as the "*ultraviolet catastrophe*"). This can be seen in the Rayleigh-Jeans curve of Fig. 3.

Planck used purely thermodynamic entropy arguments to derive an improved equation for Wien's distribution law shown in Eq. (1). His derived equation was of the form [2]

$$\rho(\nu, T) = \frac{C\nu^3}{\exp(\beta\nu/T) - 1}. \tag{12}$$

It has been suggested that Planck discovered his famous constant (h) in the evening of October 7, 1900 [1]. Planck had taken into account some additional experimental data by Heinrich Reubens and Ferdinand Kurlbaum as well as Wien's formula and he deduced in his Eq. (12), an expression that "fitted" all the available experimental data. His formula was the now known as the blackbody radiation formula given by

$$\rho(\nu, T) = \frac{8\pi\nu^2 n^3}{c^3} \frac{h\nu}{\exp(h\nu/k_B T) - 1}, \tag{13}$$

where $h = 6.62607015 \times 10^{-34} Joule \cdot sec$ is known as Planck's constant. The above expression reduces to Wien's formula for high frequencies (i.e. $h\nu/k_B T \gg 1$) and to Rayleigh-Jeans formula for low frequencies (i.e. $h\nu/k_B T \ll 1$). An example of Planck's radiation formula is shown in Fig. 3 along with Rayleigh-Jeans and Wien's approximations for a blackbody of absolute temperature $T = 6000^\circ K$.

Having obtained his formula Planck was concerned to discover its physical basis. It was hard to argue about the density of electromagnetic modes determination. Therefore, he focused on the average energy per electromagnetic mode. After discussions he had with Boltzmann regarding the number of ways of distributing discrete equal energy values among a number of molecules, Planck made the hypothesis that electromagnetic energy at frequency ν could only appear as a multiple of the step size $h\nu$ which was a quantum of energy (later it was called photon). I.e., the energy of the electromagnetic modes could be of the form $E_i = ih\nu$ where $i = 0, 1, 2, \cdots$). Energies between $ih\nu$ and $(i+1)h\nu$ do not occur. Then he used Boltzmann's statistics to compute the average energy of an electromagnetic mode. If E_0, E_1, E_2, ..., are the allowed energies then according to Boltzmann's statistics the probability of an electromagnetic mode to have an energy E_i is

$$p(E_i) = A \exp\left(-\frac{E_i}{k_B T}\right), \tag{14}$$

and the normalization constant A is given by

$$\sum_{i=0}^{\infty} p(E_i) = 1 \Longrightarrow A = \frac{1}{\sum\limits_{i=0}^{\infty} \exp(-E_i/k_B T)} = 1 - \exp\left(-\frac{h\nu}{k_B T}\right). \tag{15}$$

Then the average energy $\langle E \rangle$ of an electromagnetic mode can be determined as follows

$$\begin{aligned} \langle E \rangle &= A \sum_{i=0}^{\infty} E_i \exp\left(-\frac{E_i}{k_B T}\right) = A \left[1h\nu e^{-h\nu/k_B T} + 2h\nu e^{-2h\nu/k_B T} + \cdots\right] = \\ &= A \, \frac{h\nu \exp(-h\nu/k_B T)}{[1 - \exp(-h\nu/k_B T)]^2} = \frac{h\nu}{\exp(h\nu/k_B T) - 1}. \end{aligned} \tag{16}$$

Using the above calculation of the average energy of an electromagnetic mode the Planck's formula can be rewritten with the physical meaning of each of its terms

$$\rho(\nu, T) = \underbrace{\frac{8\pi\nu^2 n^3}{c^3}}_{\substack{\text{Number of em modes} \\ \text{per volume per frequency}}} \overbrace{h\nu}^{\text{photon energy}} \underbrace{\frac{1}{\exp(h\nu/k_B T) - 1}}_{\text{Number of photons/mode}}. \tag{17}$$

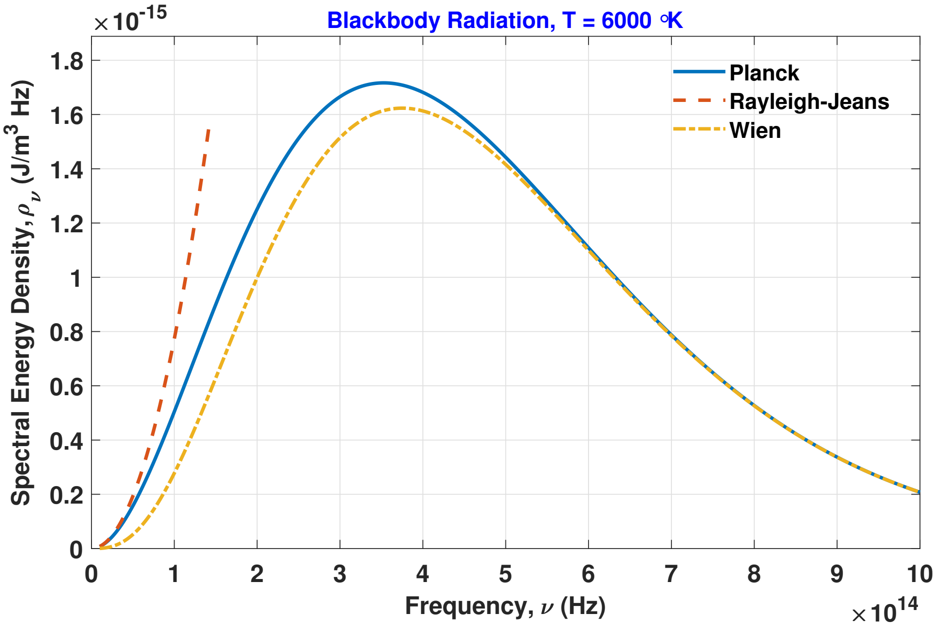

Figure 3: Blackbody radiation for $T = 6000°$ K. The initial theories by Rayleigh-Jeans and Wien are also shown for comparison.

Later Planck used the energy discretization of the quantum oscillator, i.e. $E_i = [(1/2) + i]h\nu$ $(i = 0, 1, 2, \cdots)$. Therefore, he introduced what is known today as the zero point energy, which is the lowest energy of a quantum oscillator. This lowest energy can not be zero due to the Heisenberg's uncertainty principle. In this case the average energy of an electromagnetic mode can be calculated in a similar manner as in Eq. (16) and is given by

$$\langle E \rangle = \frac{h\nu}{2} + \frac{h\nu}{\exp(h\nu/k_B T) - 1}, \tag{18}$$

However, in the above equation, the zero point energy $h\nu/2$ term causes increase to the radiation density $\rho(\nu, T)$ to infinity, and should not be used for the blackbody radiation energy density [8–14]. One simplistic approach to explain the absence of the zero energy term is that the photons that are either emitted or absorbed by the blackbody radiator are related to transitions between energy states $E_i - E_{i'} = (i - i')h\nu = \ell h\nu$ (where $\ell = 0, 1, 2, \cdots$), and consequently the initial assumption of Planck should be used as in Eq. (16). As a general comment, the zero point energy, i. e. the vacuum energy is one of the still controversial issues of modern physics. The density of electromagnetic modes can also be expressed per wavelength (freespace) and is given by

$$\frac{d\mathcal{N}(\lambda_0)}{d\lambda_0} = -\frac{8\pi n^3}{\lambda_0^4}, \tag{19}$$

and the corresponding density of electromagnetic radiation of a blackbody per wavelength (freespace) is

$$\rho(\lambda_0, T) = \frac{8\pi n^3}{\lambda_0^4} \frac{hc/\lambda_0}{\exp(hc/\lambda_0 k_B T) - 1}. \tag{20}$$

3 Blackbody Radiated Power, Radiance, and Exitance

Frequently in the literature the blackbody radiation formula is expressed in terms of the radiant exitance (or radiant emittance) of the blackbody (in units of power/area = W/m^2). The radiant exitance expresses the total power emitted by a source in a hemisphere (towards the direction of emission) per unit area of the source. The Poynting vector expresses the power per unit area of the electromagnetic radiation. Therefore, the Poynting vector is given by $P_{avg} = (1/2Z)|E|^2$ where E is the electric field amplitude of the electromagnetic wave, and $Z = \sqrt{\mu_0/n^2\epsilon_0} = Z_0/n$ (where Z_0 is the freespace wave impedance) is the intrinsic impedance of the non-magnetic homogeneous isotropic medium in which the electromagnetic radiation propagates. The energy density of the electromagnetic radiation is given by $w_{em} = (1/2)n^2\epsilon_0|E|^2$. Therefore, $P_{avg} = (c/n)w_{em}$. However, the energy density between ν and $\nu + d\nu$ (or equivalently between λ_0 and $\lambda_0 + d\lambda_0$) is $dw_{em} = \rho(\nu, T)d\nu = \rho(\lambda_0, T)d\lambda_0$ and then the power per unit area (between ν and $\nu + d\nu$ or equivalently between λ_0 and $\lambda_0 + d\lambda_0$) dP_{avg} can be determined as follows

$$dP_{avg} = \frac{8\pi n^2 \nu^2}{c^2} \frac{h\nu}{\exp(h\nu/k_B T) - 1} d\nu = P_{avg,\nu} d\nu, \tag{21}$$

$$dP_{avg} = \frac{8\pi n^2 c}{\lambda_0^4} \frac{hc/\lambda_0}{\exp(hc/\lambda_0 k_B T) - 1} d\lambda_0 = P_{avg,\lambda_0} d\lambda_0. \tag{22}$$

The radiance L (in $W/m^2 sr$ where $sr = steradian$, is discussed in the Radiometry and Photometry chapter) of a radiant source (such as a blackbody radiator) is defined as $L = d^2P/dA_\perp/d\Omega$ where d^2P is the differential electromagnetic power that is emitted by the source in a specified direction, $dA_\perp$ is the differential source area element perpendicular to the specified direction of propagation, and $d\Omega$ is the differential solid angle inside which the differential power is propagated in the specified direction [15]. A blackbody emits radiation equally in all directions and consequently it seems similarly bright from any direction observed. This means that its radiance L is constant and independent of the observation angle. Such a source is called *Lambertian* [15]. Therefore, a blackbody is always a Lambertian source. Integrating the blackbody radiance all over the solid angles it can be easily shown that $\int_\Omega L d\Omega = L\int_\Omega d\Omega = 4\pi L = \int(d^2P/dA_\perp) = P_{avg}$. Then the spectral radiance, dL_s of a blackbody radiator between ν and $\nu + d\nu$ or λ_0 and $\lambda_0 + d\lambda_0$ can be expressed as follows

$$dL_s = \frac{dP_{avg}}{4\pi} = \frac{2n^2\nu^2}{c^2}\frac{h\nu}{\exp(h\nu/k_BT)-1}d\nu = L_{s,\nu}d\nu, \qquad \text{and} \tag{23}$$

$$dL_s = \frac{dP_{avg}}{4\pi} = \frac{2n^2c}{\lambda_0^4}\frac{hc/\lambda_0}{\exp(hc/\lambda_0k_BT)-1}d\lambda_0 = L_{s,\lambda_0}d\lambda_0. \tag{24}$$

From radiometry [15] it can be easily determined that the radiance L and the radiant exitance (emittance) M (W/m^2) of a blackbody (or a Lambertian source in general) can be related from the equation $M = L\pi$. This is straightforward to show since $M = \int_\Omega[d^2P/(dA_s d\Omega)]d\Omega = \int_\Omega L\cos\theta d\Omega = \int_{\theta=0}^{\pi/2}\int_{\phi=0}^{2\pi} L\cos\theta\sin\theta d\theta d\phi = L\pi$ (where $dA_s = dA_\perp/\cos\theta$ and $d\Omega = \sin\theta d\theta d\phi$). Consequently $dM = \pi dL = M_\nu(\nu)d\nu = M_{\lambda_0}(\lambda_0)d\lambda_0 = M_\lambda(\lambda)d\lambda$, where M_ν, M_{λ_0}, and M_λ are the spectral exitances in $W/m^2/Hz$, $W/m^2/m$ (in freespace wavelength) and $W/m^2/m$ (inside medium wavelength), respectively. In addition, $c = \lambda_0\nu$ and $c/n = \lambda\nu = (\lambda_0/n)\nu$. For example, the radiant spectral exitance (power/unit area/frequency $= W/m^2/Hz$) of a blackbody radiator is given by:

$$M_\nu(\nu) = \frac{2\pi n^2\nu^2}{c^2}\frac{h\nu}{\exp(h\nu/k_BT)-1}, \tag{25}$$

while the same spectral exitance expressed per wavelength (in freespace or in medium) interval (power/unit area/wavelength $= W/m^2/m$) is given by

$$M_{\lambda_0} = \frac{2\pi n^2c}{\lambda_0^4}\frac{hc/\lambda_0}{\exp(hc/\lambda_0k_BT)-1}, \tag{26}$$

$$M_\lambda = \frac{2\pi c}{n^2\lambda^4}\frac{hc/\lambda}{\exp(hc/\lambda nk_BT)-1}. \tag{27}$$

Integrating the above equations over all frequencies (or wavelengths) the radiant exitance M of a blackbody radiator at temperature T can be determined. This is known as Stefan's law and is expressed by the following equation

$$M = \int_0^\infty M_{\lambda_0}d\lambda_0 = \Big(\frac{2\pi^5k_B^4}{15h^3c^2}\Big)n^2T^4 = \sigma n^2T^4 \tag{28}$$

where $\sigma = 5.670374419\times10^{-8}\, W/m^2\,{}^\circ K^{-4}$ = Stefan-Boltzmann constant (usually the refractive index is considered that of vacuum or air, i.e. $n \simeq 1$). The maxima of the blackbody radiator curve can be found from the solution of the equation

$$\frac{dM_{\lambda_0}(\lambda_{0,max})}{d\lambda_0} = 0 \Rightarrow \frac{hc}{\lambda_{0,max}k_BT} = 4.965114231 \Rightarrow \lambda_{0,max}T = 2897.772\,\mu m^\circ K, \tag{29}$$

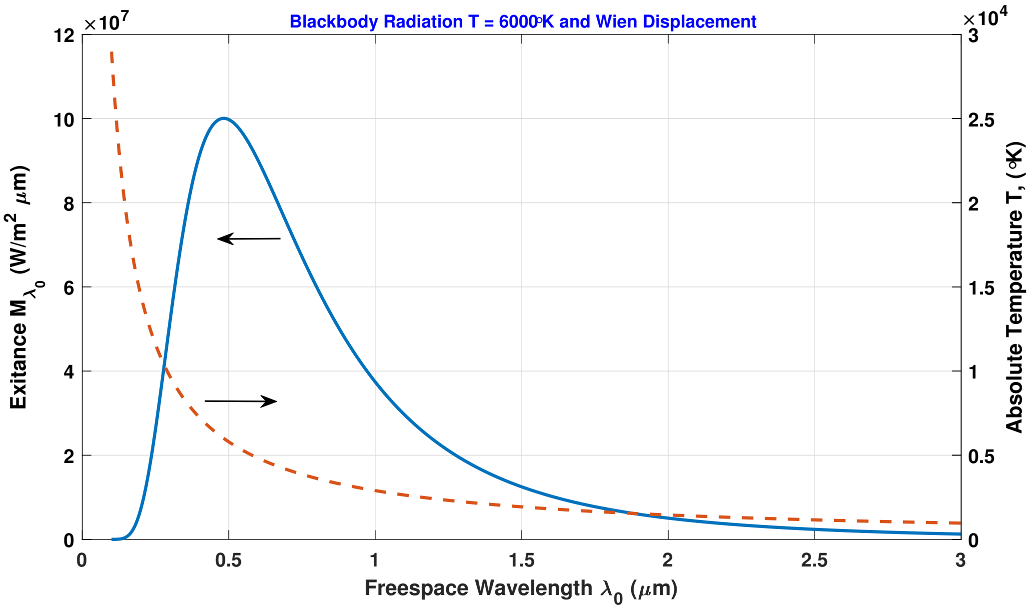

Figure 4: Blackbody radiation spectral exitance (emittance), $M_{\lambda_0}(\lambda_0)$, for $T = 6000°$ K as a function of freespace wavelength. The Wien's displacement law is also shown for the same wavelength range. The maximum of M_{λ_0} occurs for $\lambda_{0,max} = 0.483\,\mu m$.

where the last part of the above equation described how the peak of the blackbody radiation shifts with the temperature and it is known as Wien's displacement law. An example of M_{λ_0} for $T = 6000\,°$K and Wien's displacement law are shown in Fig. 4. A similar Wien's displacement law can be defined for M_ν. The maxima for M_ν can be found by

$$\frac{dM_\nu(\nu_{max})}{d\nu} = 0 \Rightarrow \frac{h\nu_{max}}{k_B T} = 2.82143937 \Rightarrow \frac{\nu_{max}}{T} = 5.878926 \times 10^{10}\,Hz/°K. \tag{30}$$

The derivation of Wien's law is presented in Appendix B with the utilization of Lambert's function. An example of M_ν for $T = 6000\,°$K and Wien's displacement law are shown in Fig. 5. It is mentioned that the peak of M_{λ_0}, $\lambda_{0,max}$, and the peak of M_ν, ν_{max}, are not related by $\lambda_{0,max}\nu_{max} = c$ since the corresponding spectral exitances are per unit wavelength and per unit frequency, respectively.

3.1 Radiance Conservation

An interesting point that should be discussed is the presence of the refractive index in Eq. (28). It is reminded that n corresponds to the refractive index (assuming no dispersion) of the medium that exists inside the blackbody cavity (see the calculation of the density of electromagnetic

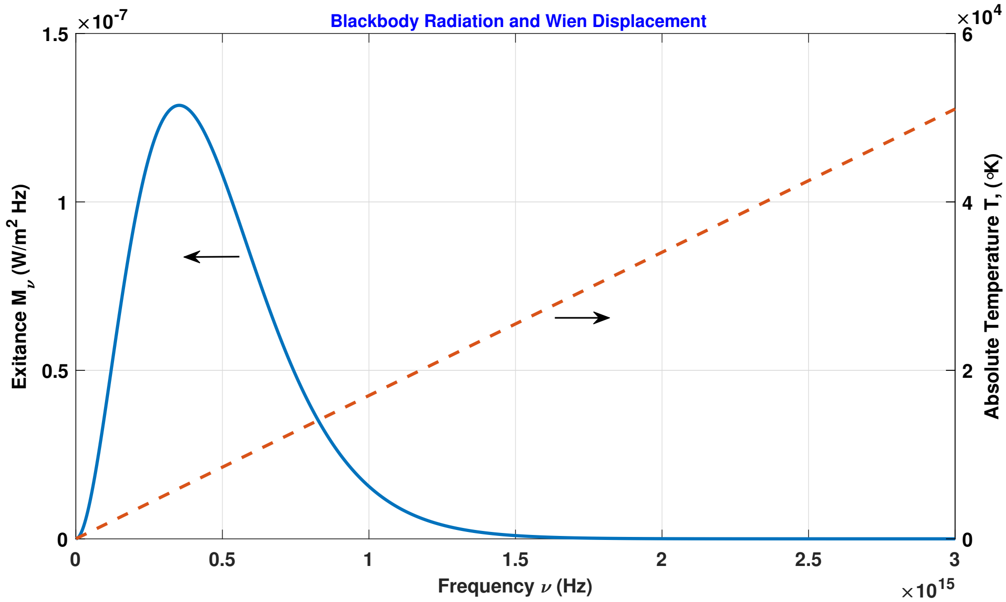

Figure 5: Blackbody radiation spectral exitance (emittance), $M_\nu(\nu)$, for $T = 6000°$ K as a function of frequency. The Wien's displacement law is also shown for the same frequency range. The maximum of M_ν occurs for $\nu_{max} = 3.52 \times 10^{14}\,Hz$.

modes inside the cuboid cavity). However, the radiated electromagnetic energy propagates away from the blackbody radiator. In many textbooks the refractive index is omitted from Eq. (28) since it is assumed that the blackbody emits radiation into vacuum or into the air (where $n_{air} \simeq 1$). This is justified because of the radiance's conservation [16, 17] between two homogeneous media of different refractive index. Let's consider a smooth boundary between two dielectric media of refractive indices of n_1 and n_2 respectively as it is shown in Fig. 6. In this figure an elementary beam of rays is incident from the left on a small area element dA of the smooth boundary [16,17]. The normal on the differential element is assumed to represent the polar axis of a coordinate system center at the middle of the differential element dA with its transverse plane being in the tangential direction of the boundary (and therefore perpendicular to the plane of the interface shown in Fig. 6). Since the boundary is assumed to be smooth the Snell's law applies for the elementary rays. Therefore, $n_1 \sin\theta_1 = n_2 \sin\theta_2$. Neglecting the reflection losses (which is definitively an approximation) the power in the beam should be the same at both sides of the boundary. I.e. $d^2P_1 = d^2P_2$. However, $d^2P_1 = L_1 \cos\theta_1 dA d\Omega_1 = L_1 \cos\theta_1 dA \sin\theta_1 d\theta_1 d\phi$ where ϕ lies in the transverse to the boundary plane. Similarly, $d^2P_2 = L_2 \cos\theta_2 dA d\Omega_2 = L_2 \cos\theta_2 dA \sin\theta_2 d\theta_2 d\phi$. Differentiating the Snell's law gives $n_1 \cos\theta_1 d\theta_1 = n_2 \cos\theta_2 d\theta_2$. In order to satisfy the power conservation the following holds

$$\begin{aligned}
d^2P_1 &= L_1 \cos\theta_1 dA \sin\theta_1 \; d\theta_1 d\phi = d^2P_2 = L_2 \cos\theta_2 dA \sin\theta_2 \; d\theta_2 d\phi \Longrightarrow \\
L_1 &= L_2 \, \frac{\cos\theta_2 \; d\theta_2}{\cos\theta_1 \; d\theta_1} \, \frac{\sin\theta_2}{\sin\theta_1} = L_2 \, \frac{n_1^2}{n_2^2} \Longrightarrow \\
\frac{L_1}{n_1^2} &= \frac{L_2}{n_2^2} \;=\; L_0 \qquad \Longleftrightarrow \qquad \frac{M_1}{n_1^2} \;=\; \frac{M_2}{n_2^2} \;=\; M_0,
\end{aligned} \tag{31}$$

where L_0 and M_0 are the radiance and exitance in vacuum respectively. Therefore, returning to Eq. (28) it is now obvious that $M_i = n_i^2 M_0$ where $M_0 = \sigma T^4$. This might imply that if $n_i > 1$ the exitance radiated from a dielectric medium into air could be larger than M_0. This is not the case since some of the energy emitted within the medium of refractive index n_i is reflected back into the emitting medium at the medium-air interface due to total internal reflection of the radiation (from Snell's law the maximum angle that is refracted into the air is $\theta_{max} = \sin^{-1}(1/n_i)$ which is the critical angle). Therefore only radiation within a cone of apex angle θ_{max} Is refracted into air (neglecting reflection losses). The radiated power for an area dA (see Fig. 6) in the accepted cone can be determined as

$$\begin{aligned}
dP &= \int_0^{2\pi} \int_0^{\theta_{max}} L_i dA \cos\theta \sin\theta d\phi d\theta = 2\pi L_i dA \frac{\sin^2\theta_{max}}{2} \\
&= \pi L_i dA \frac{1}{n_i^2} = \frac{M_i}{n_i^2} dA = M_0 dA,
\end{aligned}$$

and consequently the total power (per unit area) emitted by a blackbody radiator does not depend on the refractive index of the medium. Of course, in this analysis all reflections where neglected. Some discussion about taking into account the reflections is presented in Refs. [17,18].

4 Thermal Radiation Basics

The blackbody is an ideal radiator. The basics properties of blackbody radiation are: (a) The radiation emitted by a blackbody is isotropic, homogeneous and unpolarized, i.e. the radiation is completely diffused (b) The blackbody radiation at a given wavelength (or frequency) depends only on the temperature; (c) A blackbody emits more radiation than any other object at the same temperature. Therefore, blackbody radiation represents the upper limit to the amount of radiation that a real body may emit at a given temperature. Since a blackbody radiator is simultaneously a perfect absorber and a perfect emitter, it cab used as a reference to compare

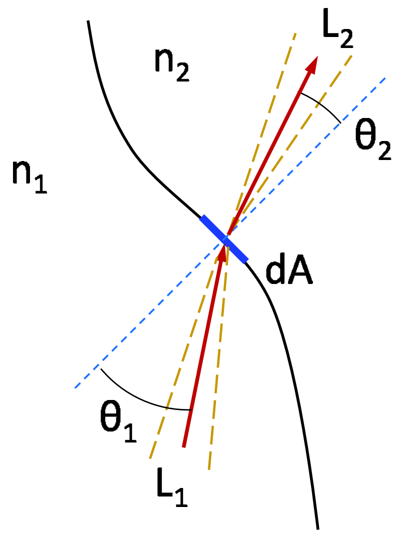

Figure 6: Radiance conservation at a smooth boundary between two homogeneous dielectric media with refractive indices n_1 and n_2 respectively.

the radiative properties of real surfaces. At any given freespace wavelength λ_0, the emissivity $\varepsilon(\lambda_0, T)$, is defined as the ratio of the actual emitted radiant exitance (or radiance) $\tilde{M}_{\lambda_0}$ (or $\tilde{L}_{\lambda_0}$) over the emitted radiant exitance of a blackbody M_{λ_0} (or L_{λ_0}),

$$\varepsilon(\lambda_0, T) = \frac{\tilde{M}_{\lambda_0}(\lambda_0, T)}{M_{\lambda_0}(\lambda_0, T)} = \frac{\tilde{L}_{\lambda_0}(\lambda_0, T)}{L_{\lambda_0}(\lambda_0, T)}. \tag{32}$$

Of course Eq. (32) holds only for Lambertian emitters where $M = L\pi$ (and L is direction independent) as it was mentioned earlier. Usually emissivity of a real object is defined using the ratio of radiances and not the exitances. This is because in real objects the radiation depends not only on the wavelength and temperature but also on the direction of emission. Therefore, the most elemental emissivity of a real object is expressed by the *spectral directional emissivity*, $\varepsilon(\lambda_0, T, \theta, \phi)$, where θ and ϕ are the polar and azimuthal angles that specify the direction [19]. When the radiance is integrated over the hemisphere of emission the *spectral hemispherical emissivity*, $\varepsilon(\lambda_0, T)$, is defined using the ratio of exitances as in Eq. (32) [19].

Emissivity is a measure of how strongly a body radiates at a given wavelength, temperature, and direction. For simplicity, from now on in this chapter the spectral hemispherical emissivity is referred as simple emissivity. Emissivity ranges between zero and one for all real substances ($0 \leq \varepsilon(\lambda_0, T) \leq 1$). A gray body (and diffused body so its radiation does not depend on direction) is defined as a substance whose emissivity is independent of wavelength, i.e. $\varepsilon(\lambda_0, T) = \varepsilon(T)$. In the atmosphere, clouds and gases have emissivities that could vary significantly with wavelength due to various absorption lines. On the other hand the ocean surface has near unit emissivity in the visible regions of the spectrum and resembles a blackbody.

For a body in local thermodynamic equilibrium the amount of thermal energy emitted must be equal to the energy absorbed. Otherwise the body would heat up or cool down in time, contrary to the assumption of equilibrium. As a result of this it can be said that materials that are strong absorbers at a given wavelength are also strong emitters at that wavelength. Similarly weak absorbers are weak emitters.

All bodies are constantly bombarded by electromagnetic radiation. When radiation is incident in slab of a semi-transparent material, as shown in Fig. 7, the fraction of the incident radiation that is reflected is called reflectivity, R, the fraction of the incident radiation that is transmitted is called transmissivity, T, and the fraction of the incident radiation that is absorbed is called absorptivity, A. Of course the reflectivity can be complicated depending on the incident angle and can be characterized either as specular (mirror-like) or diffused (equally reflected in all backward directions. The R, T, and T are assumed to be the average quantities for all directions and wavelengths of the incident radiation [19].

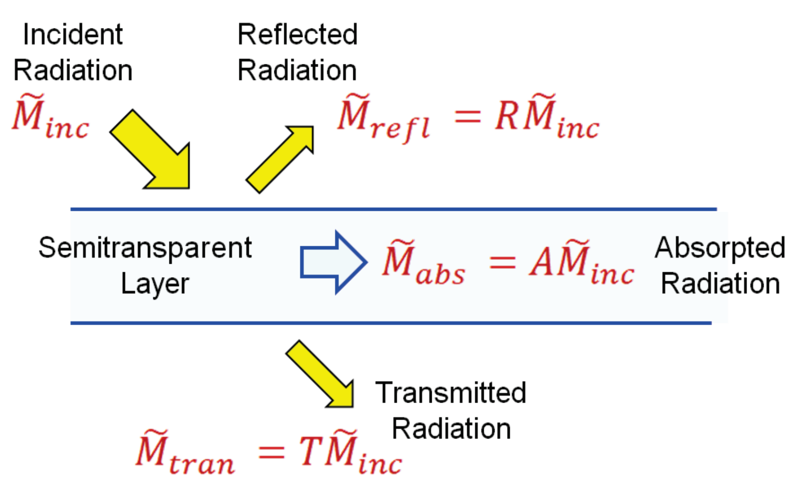

Figure 7: The incident, $\tilde{M}_{inc}$, reflected, $\tilde{M}_{refl} = R\tilde{M}_{inc}$, transmitted, $\tilde{M}_{tran} = T\tilde{M}_{inc}$, and absorbed, $\tilde{M}_{abs} = A\tilde{M}_{inc}$, powers respectively, by a semi-transparent homogeneous material slab. The R, T, and A, represent the reflectivity, transmissivity, and absorptivity, of the material, respectively.

The conservation of energy requires that R, T, and A obey the equation:

$$R + T + A = 1. \tag{33}$$

For ideal blackbodies the reflected and transmitted powers are zero, i.e., $R = T = 0$ and consequently $A = 1$. For opaque materials $T = 0$ and therefore $R + A = 1$. For semi-transparent materials like gases the reflectivity is absent, $R = 0$, and consequently $T + A = 1$.

4.1 Kirchoff's Law

Consider a small body of surface area S, temperature T, emissivity ε, and absorptivity A that is fully contained in a large isothermal volume of the same temperature T as shown in Fig. 8 [19]. The large isothermal volume can be considered a blackbody cavity and the body of surface S is too small and therefore can not affect the status of the large blackbody enclosure. The radiation incident on the small body is $M_{inc} = \sigma T^4$ according to Stefan-Boltzmann law.

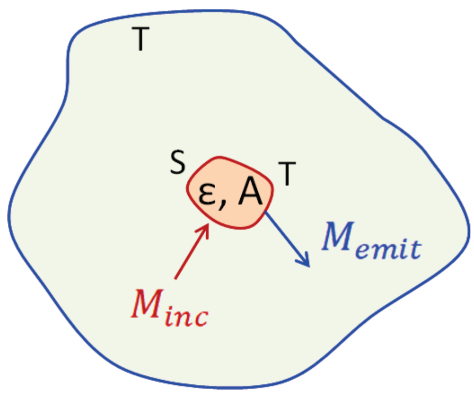

Figure 8: A small body of temperature T, surface area S, emissivity ε, and absorptivity A is inside a large isothermal enclosure of temperature T also.

The radiation absorbed by the small body is $M_{abs} = AM_{inc} = A\sigma T^4$. On the other hand, the radiation emitted by the small body is $M_{emit} = \varepsilon M_{inc} = \varepsilon\sigma T^4$. Considering thermodynamic equilibrium for the small body the the absorbed and the emitted radiation should be equal. Consequently, $A\sigma T^4 = \varepsilon\sigma T^4$, which results in what is known as the Kirchhoff's law:

$$\varepsilon(T) \;=\; A(T), \tag{34}$$

where both the emissivity as well as the absorptivity are average values over all wavelengths, and directions. In general, the Kirchhoff's law can be generalized as $\varepsilon(\lambda_0, T, \theta, \phi) = A(\lambda_0, T, \theta, \phi)$.

4.2 Color Temperature

Blackbody radiation is also used to establish a color scale as a function of the absolute temperature. The *color temperature* of a light source is the temperature of a blackbody with the closest spectral distribution with the source. However, color temperature is strictly defined for blackbody radiators since the spectral response of a blackbody is completely defined by its temperature. Real sources though do not emit blackbody spectrums. In this case it was proposed to use the *C*orrelated Color Temperature (CCT) [20, 21]. The correlated color temperature (CCT) is defined as a measure of light source color appearance by considering the proximity of the light source's chromaticity coordinates to the blackbody locus. Therefore, the CCT is used as a single number to characterize the color of a light source rather than the two chromaticity coordinates required to specify quantitatively a color. The CCT is measured in the u-v chromaticity coordinates (see Appendix C). For example, the chromaticity coordinates x, y of a light source can be determined from its spectrum and the color matching functions $\bar{x}(\lambda_0)$, $\bar{y}(\lambda_0)$, $\bar{z}(\lambda_0)$. Then the resulting x, y chromaticity coordinates are transformed in the u, v chromaticity coordinates [22] (Appendix C). If $u(T)$ and $v(T)$ are the u, v chromaticity coordinates of a blackbody radiator then the CCT of the light source of interest is defined as the temperature CCT $= T_{_{CCT}}$ that minimizes the distance of (u, v) point from the Planckian locus (which is the locus of blackbody radiators in the $u - v$ diagram. I.e., $T_{_{CCT}}$ is defined as

$$\mathrm{CCT} = T_{_{CCT}} = \min_{T} \left\{ d = \left[(u - u(T))^2 + (v - v(T))^2 \right]^{1/2} \right\}. \tag{35}$$

The above equation actually finds the intersection of the normal to the Planckian locus from point (u, v). This intersection defines CCT. Usually, on the chromaticity diagram isotemperature lines are drawn by specifying the maximum possible distance acceptable Δuv from the Planckian locus in the u-v diagram. These lines can be easily transformed into the standard x-y chromaticity diagram. For example, isotemperature lines with $\Delta uv = \pm 0.02$ are shown in Fig. 9a and 9b in the u-v and in the x-y diagrams, respectively. The isotemperature lines are shown for temperatures ranging from 1515 °K (first isotemperature line from the right) to 24959 °K (first isotemperature line from the left). The temperatures were selected to differ by $10\,mired = 10MK^{-1}$ (micro reciprocal degrees, $MK^{-1} = 10^6\,\mathrm{K}/T$) according to Ref. 23. The details of the calculation of the isotemperature lines is presented in Appendix C.

Color temperature and correlated color temperature is a characteristic of visible light only

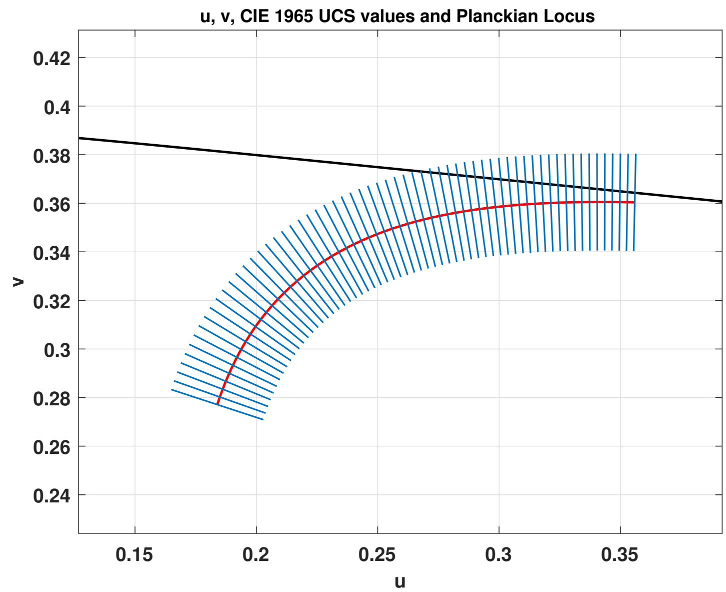

(a)

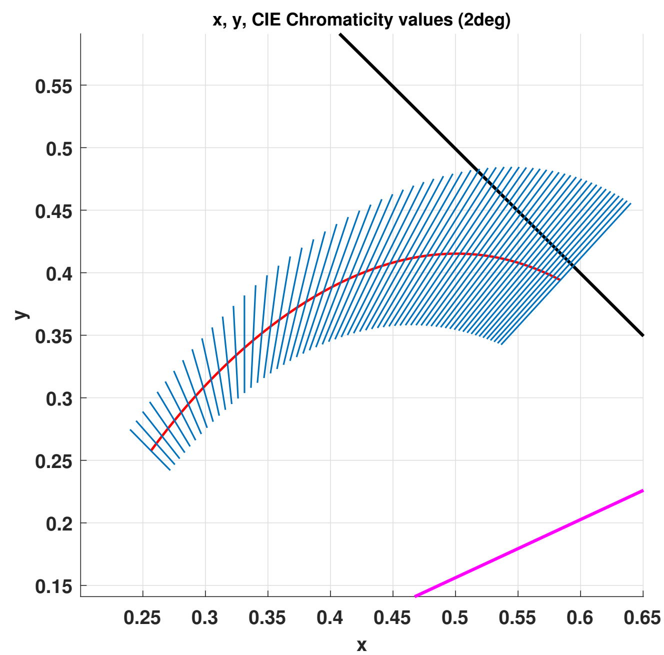

(b)

Figure 9: (a) Isotemperature lines in uv chromaticity diagram for $\Delta uv = 0.02$. The solid black line is part of the boundary of the chromaticity space. The red line is the Planckian locus. The temperatures (b) Isotemperature lines in xy chromaticity diagram for $\Delta uv = 0.02$. The solid black line is part of the boundary of the chromaticity space. The red line is the Planckian locus and the purple line is part of the *line of purples*.

and is used in various fields as in lighting, photography, publishing, manufacturing, astrophysics, and others. Correlated color temperatures above 5000° K are called "cool colors"(look bluish), while color temperatures in the range of 2700-3000° K are called "warm colors" (look yellowish). For example, the sun has a typical correlated color temperature of $\sim 5780°$ K.

5 Cosmic Microwave Background Radiation (CMB)

The discovery and measurement of the Cosmic Microwave Background radiation (CMB) is of great importance to modern cosmology since it provided critical information for the early universe such as the amount of regular matter, dark matter, and dark energy, the age of the universe, the flatness of the universe, the Hubble constant etc. The observation of the CMB radiation confirmed the "Big Bang" theory and provides a picture of the young universe. At the beginning of time the temperature of the universe was extremely high. For example, about three minutes after the Big Bang the temperature was of the order of $10^9\,{}^\circ K$! At these temperatures protons, electrons and neutrons existed along with photons and they formed an opaque plasma fog. No atoms were formed yet and photons were continuously absorbed and re-emitted but could not escape out of the plasma. It took about 380000 years for the universe to cool down to about $3000\,{}^\circ K$. At this temperature the first hydrogen and helium atoms were formed and the universe became transparent for the photons. This era is known in cosmology as photon decoupling. These early photons that escape from the young universe are still traveling today and constitute the faint CMB radiation that fills all space. Of course due to the expansion of the universe these early photons that should obey the blackbody radiation pattern for $T = 3000\,{}^\circ K$ in the present time have cool down to a temperature of about $T = 2.72548 \pm 0.00057\,{}^\circ K$ [24]! This is due to the cosmological redshift due to the expansion of the universe from the age of 380000 years to its present age of about 13.8 billion years. This observed redshift corresponds to an expansion by a factor of about 1100 since the universe initial transparency to present time [25]. These CMB photons is a picture of the early universe before even stars were formed!

The CMB radiation was first predicted in 1948 by Ralph Alpher and Robert Herman [26]. However, the first observation of the CMB radiation was made in 1964, by Arno Penzias and Robert Woodrow Wilson at the Crawford Hill location of Bell Telephone Laboratories. Penzias and Wilson used a horn antenna for radio astronomy and satellite communication experiments.

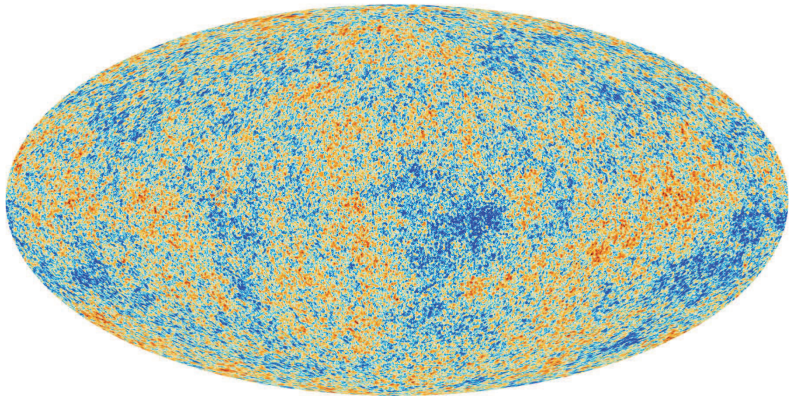

(a)

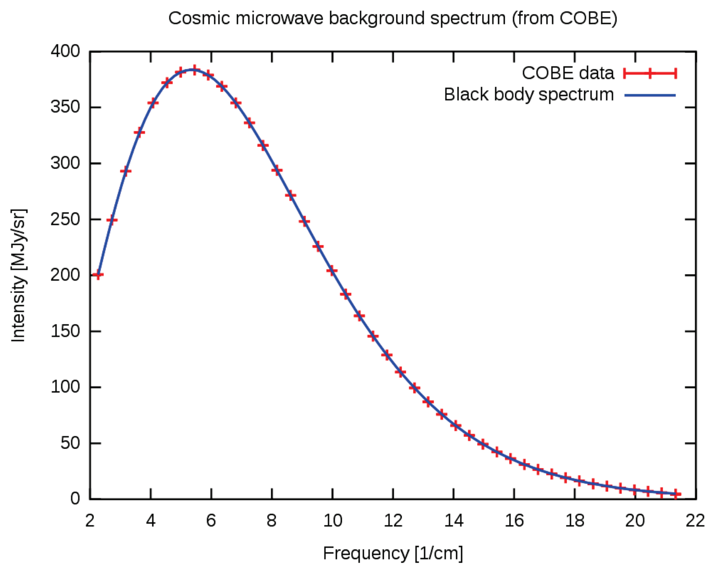

(b)

Figure 10: (a) The Cosmic Microwave Background as seen from the Planck satellite. Credit to European Space Agency (ESA). The picture, was taken from url-link: https://www.esa.int/ESA_Multimedia/Images/2013/03/Planck_CMB). (b) The cosmic microwave background radiation spectrum measured by the FIRAS instrument on the COBE satellite. This is the most precisely measured blackbody spectrum in nature. The crosses are the measurement points and the continue line is the blackbody radiation theoretical curve for $T = 2.725\,^{\circ}K$. The intensity is measured in MJy/sr where $1\,MJy = 10^6\,Jy$ and $1\,Jy = 1\,Jansky = 10^{-26}W/m^2/Hz$. (the picture, "By Quantum Doughnut - Own work, Public Domain" was taken from url-link: https://commons.wikimedia.org/w/index.php?curid=12958270).

In all their measurements and despite their efforts, they always measured a background microwave radiation which they could not account for. After discussing these results with researchers at Princeton University (R. Dicke et al.) they realized that they had measured the CMB radiation. They published their findings in 1965 [27] along with a theoretical paper by the Princeton group [28]. Penzias and Wilson were awarded the Nobel prize in Physics in 1978 for their discovery.

Since the Penzias and Wislon discovery of the CMB several much more accurate measurements were performed. In 1989, NASA (National Aeronautics and Space Agency) launched the Cosmic Background Explorer (COBE) satellite which made CMB measurements from space. Later, NASA's Wilkinson Microwave Anisotropy Probe (WMAP) in 2001, and ESA (European Space Agency) Planck in 2009, satellites made much more exact measurements of the CMB radiation. For example, the CMB radiation measurements of the most recent Planck satellite are shown in Fig. 10a. The differences in different regions of the sky are denoted by the different colors but the variations of the radiation temperature are of the order of $1/10^6 - 1/10^5$! These are called CMB radiation anisotropies and reveal the inhomogeneities of the early universe [25]. The CMB radiation measurements made by the Far Infrared Absolute Spectrometer (FIRAS) of the COBE satellite are shown in Fig. 10b. The measurements are represented by the crosses while the blackbody Planck's radiation formula for $T = 2.725\,^\circ K$ is the solid line. The CMB radiation is the most perfect blackbody radiator ever measured.

Appendices

A Determination of Electromagnetic Modes in Rectangular Metallic Cavities

The purpose of this Appendix is to review the determination of electromagnetic modes in a rectangular-shaped cavity which is considered to have perfectly conducting walls while the material filling the cavity is homogeneous, linear and isotropic [3–5]. The approach that will be presented here is rather independent from the knowledge of the solutions of rectangular metallic waveguides solutions which is normally the traditional manner in determining the cavity modes. The rectangular cavity with the corresponding coordinate system is shown in Fig. **??**. It is assumed that the determination of the TE_{mpq} modes is sought, i.e., it is assumed that $E_z = 0$ while all other field components E_x, E_y, H_x, H_y, H_z are in general nonzero. Every field component satisfies the Helmholtz equation

$$\nabla^2 S + k_0^2 n^2 S = \Big(\frac{\partial^2}{\partial x^2} + \frac{\partial^2}{\partial y^2} + \frac{\partial^2}{\partial z^2}\Big) S + k_0^2 n^2 S = 0, \tag{A.1}$$

where $S = E_x, E_y, H_x, H_y, H_z$, $k_0 = \omega/c = 2\pi/\lambda_0$ is the freespace wavenumber, and n is the refractive index of the material inside the cavity. Because of the rectangular geometry it is reasonable to seek solutions based on the method of separation of variables, i.e., $S(x, y, z) = X(x)Y(y)Z(z)$ where $X(x) = A\cos(k_x x) + B\sin(k_x x)$, $Y(y) = C\cos(k_y y) + D\sin(k_y y)$, and $Z(z) = E\cos(k_z z) + F\sin(k_z z)$, with $k_x^2 + k_y^2 + k_z^2 = k_0^2 n^2$. From the two curl Maxwell's equations $\nabla \times \vec{E} = -j\omega\mu_0\vec{H}$, and $\nabla \times \vec{H} = +j\omega\epsilon_0 n^2\vec{E}$, for the TE_{mpq} modes the following equations are derived:

$$E_x = \frac{1}{j\omega\epsilon_0 n^2}\Big(\frac{\partial H_z}{\partial y} - \frac{\partial H_y}{\partial z}\Big), \tag{A.2}$$

$$E_y = \frac{1}{j\omega\epsilon_0 n^2}\Big(\frac{\partial H_x}{\partial z} - \frac{\partial H_z}{\partial x}\Big), \tag{A.3}$$

$$E_z = \frac{1}{j\omega\epsilon_0 n^2}\Big(\frac{\partial H_y}{\partial x} - \frac{\partial H_x}{\partial y}\Big) = 0, \tag{A.4}$$

$$
\begin{aligned}
H_x &= +\frac{1}{j\omega\mu_0}\frac{\partial E_y}{\partial z}, && \text{(A.5)}\\
H_y &= -\frac{1}{j\omega\mu_0}\frac{\partial E_x}{\partial z}, && \text{(A.6)}\\
H_z &= -\frac{1}{j\omega\mu_0}\Big(\frac{\partial E_y}{\partial x} - \frac{\partial E_x}{\partial y}\Big). && \text{(A.7)}
\end{aligned}
$$

Since the cavity is surrounded by perfect conducting walls the boundary conditions on the various field components are that the normal to the wall boundary magnetic field components are zero as well as the tangential to the boundaries electric field components. These conditions can be expressed by the following equations:

$$
\begin{aligned}
H_x(x=0,y,z) &= H_x(x=a,y,z)=0, && \text{(A.8)}\\
H_y(x,y=0,z) &= H_y(x,y=b,z)=0, && \text{(A.9)}\\
H_z(x,y,z=0) &= H_z(x,y,z=d)=0, && \text{(A.10)}\\
E_x(x,y=0,z)=E_x(x,y=b,z) &= E_x(x,y,z=0)=E_x(x,y,z=d)=0, && \text{(A.11)}\\
E_y(x=0,y,z)=E_y(x=a,y,z) &= E_y(x,y,z=0)=E_y(x,y,z=d)=0, && \text{(A.12)}
\end{aligned}
$$

where it is reminded that for the TE_{mpq} modes $E_z = 0, \forall\, x, y, z$. In order to satisfy the boundary conditions for the H_x component the $X(x) = \sin(k_{xm}x)$ where $k_{xm} = (m\pi/a)$ and $m = 0, 1, \cdots$. Similarly, for H_y to satisfy the boundary conditions the $Y(y) = \sin(k_{yp}y)$ where $k_{yp} = (p\pi/b)$ and $p = 0, 1, \cdots$. Therefore, the solutions for H_x and H_y take the following form

$$
\begin{aligned}
H_x(x,y,z) &= \sin\Big(\frac{m\pi}{a}x\Big)Y_1(y)Z_1(z), \qquad \text{with } \Big(\frac{m\pi}{a}\Big)^2 + k_y^2 + k_z^2 = k_0^2n^2, && \text{(A.13)}\\
H_y(x,y,z) &= X_2(x)\sin\Big(\frac{p\pi}{b}y\Big)Z_2(z), \qquad \text{with } k_x^2 + \Big(\frac{p\pi}{b}\Big)^2 + k_z^2 = k_0^2n^2. && \text{(A.14)}
\end{aligned}
$$

In order to force the E_z field component to be zero from Eq. (A.4) the following should hold $\forall\; x, y, z,$

$$
\frac{1}{j\omega\epsilon_0 n^2}\Big\{\frac{dX_2}{dx}\sin\Big(\frac{p\pi}{b}y\Big)Z_2(z)\Big\} = \frac{1}{j\omega\epsilon_0 n^2}\Big\{\sin\Big(\frac{m\pi}{a}x\Big)\frac{dY_1}{dy}Z_1(z)\Big\} \quad \forall x,y,z. \qquad \text{(A.15)}
$$

Using $X_2(x) = A_2\cos(k_x x) + B_2\sin(k_x x)$ and $Y_1(y) = C_1\cos(k_y y) + D_1\sin(k_y y)$ it is straightforward to show that $B_2 = 0 = D_1$, and $k_x = (m\pi/a)$, $k_y = (p\pi/b)$, and the coefficients of the $Z_1(z)$ and $Z_2(z)$ are related in such a way that the field components H_x and H_y are expressed by the following equations:

$$H_x(x,y,z) = \sin\left(\frac{m\pi}{a}x\right)\cos\left(\frac{p\pi}{b}y\right)[E_1\cos(k_z z) + F_1\sin(k_z z)], \tag{A.16}$$

$$H_y(x,y,z) = \cos\left(\frac{m\pi}{a}x\right)\sin\left(\frac{p\pi}{b}y\right)\frac{p\pi/b}{m\pi/a}[E_1\cos(k_z z) + F_1\sin(k_z z)], \tag{A.17}$$

where, of course $(m\pi/a)^2 + (p\pi/b)^2 + k_z^2 = k_0^2 n^2$. Now in order to satisfy the boundary condition for the H_z field component the following solution is valid

$$H_z(x,y,z) = H_{0z}X_3(x)Y_3(y)\sin\left(\frac{q\pi}{d}z\right). \tag{A.18}$$

From the z-dependence of H_z it is implied that the E_x and E_y field components have the following form due to Eq. (A.7)

$$E_x(x,y,z) = E_{0x}X_1(x)Y_1(y)\sin\left(\frac{q\pi}{d}z\right), \tag{A.19}$$

$$E_y(x,y,z) = E_{0y}X_2(x)Y_2(y)\sin\left(\frac{q\pi}{d}z\right), \tag{A.20}$$

where E_{0x}, E_{0y} are amplitude constants. Then applying Eqs. (A.5) and (A.6) for the H_x and H_y components respectively, in conjunction with Eqs. (A.16). (A.17), (A.19), and (A.20), the following conditions must be satisfied $\forall\ x, y, z$,

$$\sin\left(\frac{m\pi}{a}x\right)\cos\left(\frac{p\pi}{b}y\right)[E_1\cos(k_z z) + F_1\sin(k_z z)] = +\frac{1}{j\omega\mu_0}\left[E_{0y}\frac{q\pi}{d}\cos\left(\frac{q\pi}{d}z\right)X_2(x)Y_2(y)\right],$$

$$\cos\left(\frac{m\pi}{a}x\right)\sin\left(\frac{p\pi}{b}y\right)\frac{p\pi/b}{m\pi/a}[E_1\cos(k_z z) + F_1\sin(k_z z)] = -\frac{1}{j\omega\mu_0}\left[E_{0x}\frac{q\pi}{d}\cos\left(\frac{q\pi}{d}z\right)X_1(x)Y_1(y)\right].$$

From the last two equations the following solutions for the E_x, E_y, H_x, H_y fields can be obtained

$$H_x = \frac{E_{0y}}{j\omega\mu_0}\left(\frac{q\pi}{d}\right)\sin\left(\frac{m\pi}{a}x\right)\cos\left(\frac{p\pi}{b}y\right)\cos\left(\frac{q\pi}{d}z\right), \tag{A.21}$$

$$H_y = \frac{E_{0y}}{j\omega\mu_0}\frac{p\pi/b}{m\pi/a}\left(\frac{q\pi}{d}\right)\cos\left(\frac{m\pi}{a}x\right)\sin\left(\frac{p\pi}{b}y\right)\cos\left(\frac{q\pi}{d}z\right), \tag{A.22}$$

$$E_x = -E_{0y}\frac{p\pi/b}{m\pi/a}\cos\left(\frac{m\pi}{a}x\right)\sin\left(\frac{p\pi}{b}y\right)\sin\left(\frac{q\pi}{d}z\right), \tag{A.23}$$

$$E_y = E_{0y}\sin\left(\frac{m\pi}{a}x\right)\cos\left(\frac{p\pi}{b}y\right)\sin\left(\frac{q\pi}{d}z\right). \tag{A.24}$$

The last component to be determined is the H_z. Using the solutions for E_x and E_y as well as Eq. (A.7) and Eq. (A.18) the following solution for H_z is obtained

$$H_z = -\frac{E_{0y}}{j\omega\mu_0}\frac{a}{m\pi}\left[\left(\frac{m\pi}{a}\right)^2 + \left(\frac{p\pi}{b}\right)^2\right]\cos\left(\frac{m\pi}{a}x\right)\cos\left(\frac{p\pi}{b}y\right)\sin\left(\frac{q\pi}{d}z\right). \tag{A.25}$$

In order to write the equations in the usual format [4,5] found in the literature the coefficient of the H_z component can be defined as $C = -(E_{0y}/j\omega\mu_0)(a/m\pi)k_c^2$ where $k_c^2 = (m\pi/a)^2 + (p\pi/b)^2$. Using C as the free parameter in the expressions of the fields of the TE_{mpq} mode the fields are summarized in the following form:

$\underline{TE_{mpq}\ \text{Modes :}}$

$$E_x = C\frac{j\omega\mu_0}{k_c^2}\left(\frac{p\pi}{b}\right)\cos\left(\frac{m\pi}{a}x\right)\sin\left(\frac{p\pi}{b}y\right)\sin\left(\frac{q\pi}{d}z\right), \tag{A.26}$$

$$E_y = -C\frac{j\omega\mu_0}{k_c^2}\left(\frac{m\pi}{a}\right)\sin\left(\frac{m\pi}{a}x\right)\cos\left(\frac{p\pi}{b}y\right)\sin\left(\frac{q\pi}{d}z\right), \tag{A.27}$$

$$E_z = 0, \tag{A.28}$$

$$H_x = -C\frac{1}{k_c^2}\left(\frac{m\pi}{a}\right)\left(\frac{q\pi}{d}\right)\sin\left(\frac{m\pi}{a}x\right)\cos\left(\frac{p\pi}{b}y\right)\cos\left(\frac{q\pi}{d}z\right), \tag{A.29}$$

$$H_y = -C\frac{1}{k_c^2}\left(\frac{p\pi}{b}\right)\left(\frac{q\pi}{d}\right)\cos\left(\frac{m\pi}{a}x\right)\sin\left(\frac{p\pi}{b}y\right)\cos\left(\frac{q\pi}{d}z\right), \tag{A.30}$$

$$H_z = C\cos\left(\frac{m\pi}{a}x\right)\cos\left(\frac{p\pi}{b}y\right)\sin\left(\frac{q\pi}{d}z\right). \tag{A.31}$$

In exactly similar manner the solutions of the TM_{mpq} modes can be calculated where the $H_z = 0$. These solutions are summarized next for completeness.

$\underline{TM_{mpq}\ \text{Modes :}}$

$$E_x = -D\frac{1}{k_c^2}\left(\frac{m\pi}{a}\right)\left(\frac{q\pi}{d}\right)\cos\left(\frac{m\pi}{a}x\right)\sin\left(\frac{p\pi}{b}y\right)\sin\left(\frac{q\pi}{d}z\right), \tag{A.32}$$

$$E_y = -D\frac{1}{k_c^2}\left(\frac{p\pi}{b}\right)\left(\frac{q\pi}{d}\right)\sin\left(\frac{m\pi}{a}x\right)\cos\left(\frac{p\pi}{b}y\right)\sin\left(\frac{q\pi}{d}z\right), \tag{A.33}$$

$$E_z = D\sin\left(\frac{m\pi}{a}x\right)\sin\left(\frac{p\pi}{b}y\right)\cos\left(\frac{q\pi}{d}z\right), \tag{A.34}$$

$$H_x = D\frac{j\omega\epsilon_0 n^2}{k_c^2}\left(\frac{p\pi}{b}\right)\sin\left(\frac{m\pi}{a}x\right)\cos\left(\frac{p\pi}{b}y\right)\cos\left(\frac{q\pi}{d}z\right), \tag{A.35}$$

$$H_y = -D\frac{j\omega\epsilon_0 n^2}{k_c^2}\left(\frac{m\pi}{a}\right)\cos\left(\frac{m\pi}{a}x\right)\sin\left(\frac{p\pi}{b}y\right)\cos\left(\frac{q\pi}{d}z\right), \tag{A.36}$$

$$H_z = 0. \tag{A.37}$$

where now D has been selected as the free parameter coefficient. For both TE_{mpq} and TM_{mpq} modes the dispersion relation and the corresponding resonance frequencies are given by the following equations

$$k_0^2 n^2 = \left(\frac{m\pi}{a}\right)^2 + \left(\frac{p\pi}{b}\right)^2 + \left(\frac{q\pi}{d}\right)^2, \tag{A.38}$$

$$\omega_{mnq} = \frac{c}{n}\sqrt{\left(\frac{m\pi}{a}\right)^2 + \left(\frac{p\pi}{b}\right)^2 + \left(\frac{q\pi}{d}\right)^2}. \tag{A.39}$$

B Lambert Function

Let the function $y = f(x) = xe^x$ and its inverse $x = f^{-1}(y) = W(xe^x)$. The inverse function $W(xe^x) = x$ is known as the Lambert function [29, 30]. A graphical representation of $W(x)$ is shown in Fig. B.1. It is straightforward to show that the function W is defined in the interval

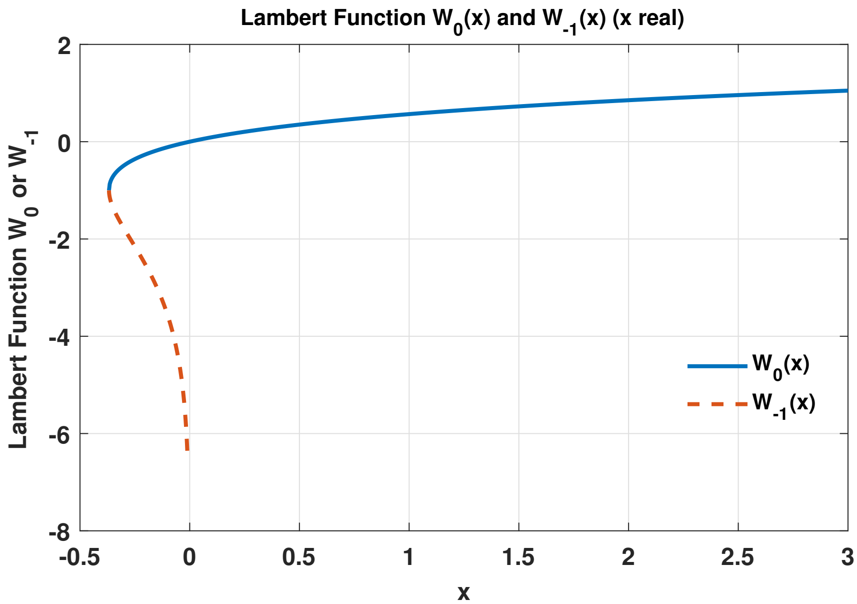

Figure B.1: Lambert function $W(x)$ showing only the real branches. The solid line corresponds to the $W_0(x)$-branch while the dash line corresponds to $W_{-1}(x)$-branch.

$-1/e \leq x \leq \infty$. In the interval $-1/e \leq x \leq 0$ there are two possible solutions that are characterized as the branches W_0 and W_{-1}. Of course the Lambert function can be extended into the complex domain with infinite number of branches W_k with k an integer. However, here the interest is on the real solutions that are represented by the branches W_0 and W_{-1}. The Lambert function is now available in several computing platforms as *Maple*, *Mathematica*, *Matlab* and others. Using the Lambert function solutions to transcendental equations of some type can be found. A general transcendental equation of the form $a^{bx} = cx + d$ (where $a > 0$) can be solved [30]. In order to solve this equation the transformation $-t = bx + bd/c$, can be utilized. In this case the equation becomes,

$$a^{bx} \;=\; cx + d \implies a^{-t-bd/c} = \frac{c}{b}\left(-t - \frac{bd}{c}\right) + d = -\frac{tc}{b} \implies$$

$$\begin{aligned}
a^{-t-(bd/c)} &= -\frac{tc}{b} \implies ta^t = -\frac{b}{c}a^{-(bd/c)} \implies \\
te^{t\ln a} &= -\frac{b}{c}a^{-(bd/c)} \implies t(\ln a)e^{t\ln a} = -(\ln a)\frac{b}{c}a^{-(bd/c)} \implies \\
t\ln a &= W\left(-(\ln a)\frac{b}{c}a^{-(bd/c)}\right) \implies \\
-t &= -\frac{1}{\ln a}W\left(-(\ln a)\frac{b}{c}a^{-(bd/c)}\right) \implies \\
bx+\frac{bd}{c} &= -\frac{1}{\ln a}W\left(-(\ln a)\frac{b}{c}a^{-(bd/c)}\right) \implies \\
x &= -\frac{d}{c}-\frac{1}{b\ln a}W\left(-(\ln a)\frac{b}{c}a^{-(bd/c)}\right). \qquad \text{(B.1)}
\end{aligned}$$

If x is replaced by $x' = -x$ the equation becomes $a^{-bx'} = (-c)x' + d$ and the Eq. (B.1) becomes

$$x' = \frac{d}{c} + \frac{1}{b\ln a}W\left(-(\ln a)\frac{b}{c}a^{-(bd/c)}\right) \qquad \text{(B.2)}$$

With the above information th Wien's law can be easily verified [Eq. (29)]. The maximum exitance can be determined from Eq. (26) taking the derivative $dM_{\lambda_0}/d\lambda_0 = 0$. Setting $x' = hc/\lambda_0 k_B T$ the derivative can be computed as $dM_{\lambda_0}/d\lambda_0 = (dM_{\lambda_0}/dx)(dx/d\lambda_0) = 0 \implies Ax'^6(5e^{x'} - 5 - x'e^{x'}) = 0$, where A a constant. Therefore, the maximum can be found from the solution of the transcendental equation $5e^{x'} - 5 - x'e^{x'} = 0 \implies e^{-x'} = (-1/5)x' + 1$. Applying Eq. (B.2) for $a = e = \exp(1)$, $b = 1$, $c = 1/5$, $d = 1$, the following solution is found:

$$x'_m = 5 + W_0(-5e^{-5}) = 4.965114231744276 \implies \lambda_{0,max}T = \frac{k_B x'_m}{hc} = 2897.721\,\mu m\,^\circ K.$$

Similarly, starting from Eq. (25) the maximum exitance in terms of frequency can be found from the zero of the derivative $dM_\nu/d\nu = 0$. Setting $x' = h\nu/k_B T$ the derivative zeroes for $A(3e^{x'} - 3 - x'e^{x'}) = 0 \implies e^{-x'} = (-1/3)x' + 1$. Applying Eq. (B.2) for $a = e = \exp(1)$, $b = 1$, $c = 1/3$, $d = 1$, the following solution is found:

$$x'_m = 3 + W_0(-3e^{-3}) = 2.821439372122079 \implies \frac{\nu_{max}}{T} = \frac{k_B x'_m}{h} = 5.878926\times 10^{10}\,Hz/^\circ K.$$

C Isotemperature Lines Calculation

The isotemperatures lines were proposed initially by Judd [20] and they were defined in the u-v chromaticity diagram proposed by MacAdam [31]. In this Appendix a simple method is presented for the computation of the isotemperature lines. The u-v chromaticity coordinates are related to the x-y chromaticity coordinates (or the X, Y, and Z tristimulus values) via the following relations [31]:

$$u = \frac{4x}{-2x + 12y + 3} = \frac{4X}{X + 15Y + 3Z}, \tag{C.1}$$

$$v = \frac{6y}{-2x + 12y + 3} = \frac{6Y}{X + 15Y + 3Z}. \tag{C.2}$$

Let a point (u, v) in the u-v chromaticity coordinates diagram as shown in Fig. C.1. This point can be represented by the position vector $\vec{r} = u\hat{\imath}_u + v\hat{\imath}_v$. The locus of points that correspond to a blackbody radiator of temperature T can easily be calculated in the x-y chromaticity diagram starting with the computation of the X, Y, and Z tristimulus values:

$$\begin{aligned} X(T) &= k \int M_{\lambda_0}(\lambda_0, T)\bar{x}(\lambda_0) d\lambda_0, \\ Y(T) &= k \int M_{\lambda_0}(\lambda_0, T)\bar{y}(\lambda_0) d\lambda_0, \\ Z(T) &= k \int M_{\lambda_0}(\lambda_0, T)\bar{x}(\lambda_0) d\lambda_0, \end{aligned}$$

for each temperature T. The term $M_{\lambda_0}(\lambda_0, T)$ is the blackbody radiant exitance [Eq, (26)], the $\bar{x}, \bar{y}, \bar{z}$ are the color matching functions, and λ_0 is the freespace wavelength. Then the chromaticities coordinates $x(T)$ and $y(T)$ can be determined from $x(T) = X(T)/[X(T) + Y(T) + Z(T)]$ and $y(T) = X(T)/[X(T) + Y(T) + Z(T)]$, respectively. Using Eqs. (C.1) and (C.2) the values of $(u(T), v(T))$ corresponding to the points of the Planckian locus can be determined. A part of this Planckian locus is shown in Fig. C.1 by the red solid line.

The Planckian locus can be represented by the vector $\vec{f}(T) = u(T)\hat{\imath}_u + v(T)\hat{\imath}_v$. This is a parametric representation of the Planckian locus via the temperature T. The normal from point (u, v) to the Planckian locus, the isotemperature line at T, is represented by the vector $\vec{r}_{uv}$ which is sought. The tangential unit vector at the intersection of the isotemperature line with the Planckian locus is $\hat{\imath}_{f'} = \vec{f}'/|\vec{f}'|$ with $\vec{f}' = d\vec{f}/dT$. Then the tangential and the normal

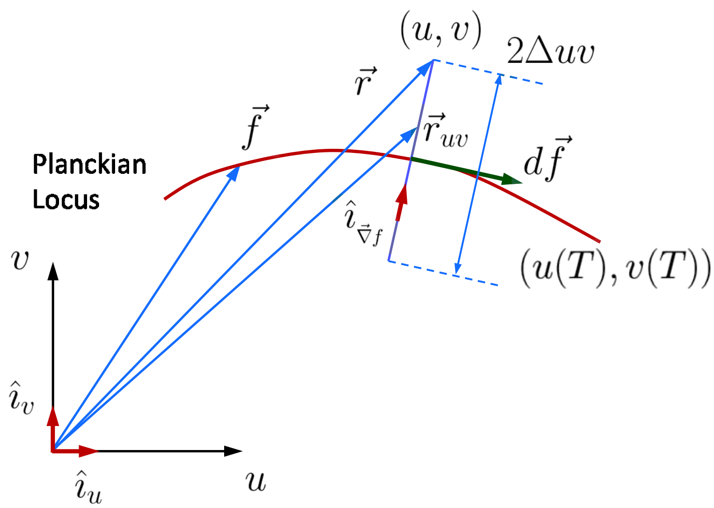

Figure C.1: Diagram used for the isotemperature line determination. The solid red line is the Planckian locus in the u-v chromaticity diagram. The line specified by $\vec{r}_{uv}$ is one isotemperature line which is perpendicular to the Planckian locus at the CCT of light source represented by (u, v) point.

unit vectors at the intersection of the isotemperature line with the Planckian locus are given by:

$$\begin{aligned}
\hat{\imath}_{f'} = \frac{\vec{f'}}{|\vec{f'}|} &= a_u \hat{\imath}_u + a_v \hat{\imath}_v, \qquad \text{with,} \\
a_u &= \frac{du(T)}{dT}, \qquad \text{and} \qquad a_v = \frac{dv(T)}{dT}, \\
\hat{\imath}_{\vec{\nabla} f} &= -a_v \hat{\imath}_u + a_u \hat{\imath}_v = -\frac{dv(T)}{dT} \hat{\imath}_u + \frac{du(T)}{dT} \hat{\imath}_v.
\end{aligned}$$

Then the isotemperature line can be described by the following expression

$$\begin{aligned}
\vec{r}_{uv}(T, t) &= u_{ISO}(T, t) \hat{\imath}_u + v_{ISO}(T, t) \hat{\imath}_v \\
&= u(T) \hat{\imath}_u + v(T) \hat{\imath}_v + \hat{\imath}_{\vec{\nabla} f} (\Delta uv) t, \qquad \text{(C.3)}
\end{aligned}$$

where t a parameter taking values in the interval $t \in [-1, 1]$ and Δuv the maximum acceptable distance of the chromaticity point (u, v) from the Planckian locus at temperature T (which is the point's correlated color temperature, CCT). The $u_{ISO}(T, t)$ and $v_{ISO}(T, t)$ are the chromaticity coordinates of the isotemperature line of temperature T. The required derivatives du/dT and dv/dT can be determined from the following expressions [by differentiating Eqs. (C.1) and

(C.2)]:

$$\begin{aligned} u'(T) = \frac{du}{dT} &= \frac{4X'(T)\,[X(T)+15Y(T)+3Z(T)] - 4X(T)\,[X'(T)+15Y'(T)+3Z'(T)]}{[X(T)+15Y(T)+3Z(T)]^2}, \\ v'(T) = \frac{dv}{dT} &= \frac{6Y'(T)\,[X(T)+15Y(T)+3Z(T)] - 6Y(T)\,[X'(T)+15Y'(T)+3Z'(T)]}{[X(T)+15Y(T)+3Z(T)]^2}, \end{aligned}$$

where the $W'(T)$ ($W = X, Y, Z$) are calculated from the following equations:

$$\begin{aligned} W'(T) &= k \int \frac{M_{\lambda_0}(\lambda_0, T)}{dT} \bar{w}(\lambda_0) d\lambda_0, \\ \frac{M_{\lambda_0}(\lambda_0, T)}{dT} &= \frac{2\pi h^2 c^3}{\lambda_0^6 k_B} \frac{1}{\left(e^{hc/\lambda_0 k_B T} - 1\right)^2}\; e^{hc/\lambda_0 k_B T} \frac{1}{T^2}, \end{aligned}$$

where $\bar{w}(\lambda_0)$ ($\bar{w} = \bar{x}, \bar{y}, \bar{z}$) are the color matching functions. Then the points of the isotemperature line at T can be transformed into the x-y chromaticity diagram via the Eqs. (C.1) and (C.2) which are converted to express x and y as functions of u and v:

$$x = \frac{3u}{2(u - 4v + 2)}, \tag{C.4}$$

$$y = \frac{v}{u - 4v + 2}. \tag{C.5}$$

Two isotemperature lines for $T = 2500\,^\circ$K and $T = 5000\,^\circ$K, with $\Delta uv = 0.02$ are shown in Fig. C.2. The isotemperature lines shown in Figs. 9a and 9b are shown both in the u-v and in the x-y coordinates. It is apparent that in the u-v diagram the isotemperature lines are normal to the Planckian locus as expected from their definition. The temperatures selected in Figs. 9a and 9b are according to the work of Kelly in Ref. 23 where the difference between the isotemperature lines was selected according to the inverse temperature difference as it was proposed initially by Priest in Ref. 32. Actually, these isotemperature lines were selected to differ successively by $10\,MK^{-1}$ (microreciprocal degrees). I.e., the initial temperature was selected to be $T_0 = 1515\,^\circ$K and the rest of the temperatures were selected by the rule:

$$10^6 \left(\frac{1}{T_i} - \frac{1}{T_{i+1}} \right) = 10\,MK^{-1},$$

where $i = 0, 1, \cdots, 62$. According to this scheme the highest isotemperature line (first from the left) is $T = 19974\,^\circ$K. A more practical problem is that given a source's chromaticity coordinates to determine its CCT. The interested reader should consult Refs. 21, 33–35 among many available, for more details on this subject.

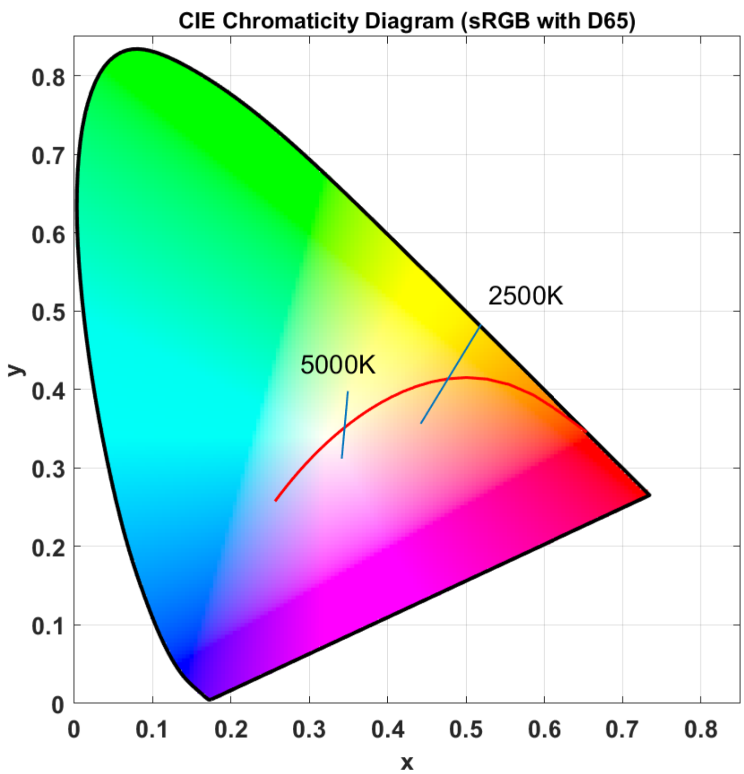

Figure C.2: The CIE 1931 chromaticity diagram with the Planckian locus. Two sample isotemperature lines are shown for temperatures 2500 °K and 5000 °K and $\Delta uv = \pm 0.02$.

References

[1] J. Baggott, *The Meaning of Quantum Theory.* New York: Oxford University Press, 1992.

[2] J. Crepeau, "A brief history of the T^4 radiation law," in *Proceedings of ASME: Heat Transfer in Energy Systems; Thermophysical Properties; Heat Transfer Equipment; Heat Transfer in Electronic Equipment*, vol. 1, (San Francisco, CA), pp. HT2009–88060, Heat Transfer Summer Conference, ASME, Jul. 19–23, 2009.

[3] C. A. Balanis, *Advanced Engineering Electromagnetics.* New York: John Wiley & Sons, Inc., 2nd ed., 2012.

[4] D. K. Cheng, *Fields and Waves in Electromagnetics.* New York: Addison Wesley, 2nd ed., 1989.

[5] S. Ramo, J. R. Whinnery, and T. Van Duzer, *Fields and Waves in Communications Electronics.* New York: John Wiley and Sons, Inc., 3rd ed., 1993.

[6] J. T. Verdeyen, *Laser Electronics.* New Jersey: Prentice Hall, 3rd ed., 1995.

[7] O. Svelto, *Principles of Lasers.* New York: Springer, Inc., 5th ed., 2010.

[8] J. L. Jiménez, L. de la Peña, and T. A. Brody, "Zero point term in cavity radiation," *Amer. J. Phys.*, vol. 48, no. 10, pp. 840–846, 1980.

[9] L. de la Peña and A. M. Cetto, "Plancks law as a consequence of the zeropoint radiation field," *Rev. Mex. Fis. (Suppl. 1)*, vol. 48, pp. 1–8, Sept. 2002.

[10] H. Vic Dannon, "Zero point energy: Planck radiation law," *Gauge Institute Journal*, vol. 1, Aug. 2005.

[11] F. Ogiba, "Plancks radiation law: Thermal excitations of vacuum induced fluctuations," *Progr. Phys.*, vol. 11, no. 2, pp. 146–148, 2015.

[12] L. Reggiani and E. Alfinito, "The puzzling of zero-point energy contribution to black-body radiation spectrum: The role of Casimir force," *Fluctuation and Noise Letters*, vol. 16, no. 04, p. 1771002, 2017.

[13] T. H. Boyer, "Blackbody radiation in classical physics: A historical perspective," *Amer. J. Phys.*, vol. 86, no. 7, pp. 495–509, 2018.

[14] T. H. Boyer, "Thermodynamics of the harmonic oscillator: derivation of the planck blackbody spectrum from pure thermodynamics," *Eur. J. Phys.*, vol. 40, p. 025101, Jan. 2019.

[15] W. L. Wolfe, *Introduction to Radiometry.* Tutorial Texts in Optical Engineering, vol. TT29, Bellingham, WA, USA: SPIE Press, 1998.

[16] F. Grunn and R. J. Becherer, *Optical Radiation Measurements, Volume 1, Radiometry.* New York: Academic Press, Inc., 1979.

[17] J. R. Howell, M. P. Mengüç, and R. Siegel, *Thermal Radiation Heat Transfer*, ch. 17. Boca Raton, FL, USA: CRC Press, Taylor & Francis Group, 6th ed., 2016.

[18] J. Hartmann, "Correct consideration of the index of refraction using blackbody radiation," *Opt. Express*, vol. 14, pp. 8121–8126, Sep. 2006.

[19] Y. A. Çengel and A. J. Ghajar, *Heat and Mass Transfer: Fundamentals and Applications*, ch. 12. New York: McGraw-Hill Education, 5th ed., 2015.

[20] D. B. Judd, "Estimation of chromaticity differences and nearest color temperature on the standard 1931 ici colorimetric coordinate system*," *J. Opt. Soc. Am.*, vol. 26, pp. 421–426, Nov. 1936.

[21] D. L. MacAdam, "Correlated color temperature?," *J. Opt. Soc. Am.*, vol. 67, pp. 839–840, June 1977.

[22] CIE, "Colorimetry," *Commission Internationale de l'Eclairage Proceedings (CIE)*, 2004. Technical Report CIE:15:2004 (CIE Central Bureau, Vienna).

[23] K. L. Kelly, "Lines of constant correlated color temperature based on MacAdam's (u,v) uniform chromaticity transformation of the cie diagram," *J. Opt. Soc. Am.*, vol. 53, pp. 999–1002, Aug. 1963.

[24] D. J. Fixsen, "The temperature of the Cosmic Microwave Background," *Astrophys. J.*, vol. 707, pp. 916–920, nov 2009.

[25] E. Gawiser and J. Silk, "The cosmic microwave background radiation," *Phys. Rep.*, vol. 333-334, pp. 245–267, 2000.

[26] R. A. Alpher and R. Herman, "Evolution of the universe," *Nature*, vol. 162, pp. 774–775, Nov. 1948.

[27] A. A. Penzias and R. W. Wilson, "A measurement of excess antenna temperature at 4080 Mc/s," *Astrophys. J.*, vol. 142, pp. 419–421, Jul. 1965.

[28] R. H. Dicke, P. J. E. Peebles, P. G. Roll, and D. T. Wilkinson, "Cosmic black-body radiation," *Astrophys. J.*, vol. 142, pp. 414–419, Jul. 1965.

[29] R. M. Corless, G. H. Gonnet, D. E. G. Hare, D. J. Jeffrey, and D. E. Knuth, "On the Lambert W function," *Adv. Comp. Math.*, vol. 5, pp. 329–359, Dec. 1996.

[30] T. Dence, "A brief look into the Lambert W function," *Applied Mathematics*, vol. 4, no. 6, pp. 887–892, 2013.

[31] D. L. MacAdam, "Projective transformations of I. C. I. color specifications," *J. Opt. Soc. Am.*, vol. 27, pp. 294–299, Aug. 1937.

[32] I. G. Priest, "A proposed scale for use in specifying the chromaticity of incandescent illuminants and various phases of daylight∗," *J. Opt. Soc. Am.*, vol. 23, pp. 41–45, Feb. 1933.

[33] M. Krystek, "An algorithm to calculate correlated colour temperature," *Color Res. & Appl.*, vol. 10, no. 1, pp. 38–40, 1985.

[34] J. Hernández-Andrés, R. L. Lee, and J. Romero, "Calculating correlated color temperatures across the entire gamut of daylight and skylight chromaticities," *Appl. Opt.*, vol. 38, pp. 5703–5709, Sept. 1999.

[35] C. Li, G. Cui, M. Melgosa, X. Ruan, Y. Zhang, L. Ma, K. Xiao, and M. R. Luo, "Accurate method for computing correlated color temperature," *Opt. Express*, vol. 24, pp. 14066–14078, June 2016.